Downloaded from orbit.dtu.dk on: May 04, 2023

DTU Library

Full Scale Measurements and CFD Investigations of a Wall Radiant Cooling System Based on Plastic Capillary Tubes in Thin Concrete Walls

Mikeska, Tomás; Fan, Jianhua; Svendsen, Svend

Published in:
Energy and Buildings

Link to article, DOI:
10.1016/j.enbuild.2017.01.033

Publication date:
2017

Document Version
Peer reviewed version

Link back to DTU Orbit

Citation (APA):
Mikeska, T., Fan, J., & Svendsen, S. (2017). Full Scale Measurements and CFD Investigations of a Wall Radiant Cooling System Based on Plastic Capillary Tubes in Thin Concrete Walls. *Energy and Buildings*, *139*, 242-253. https://doi.org/10.1016/j.enbuild.2017.01.033

General rights
Copyright and moral rights for the publications made accessible in the public portal are retained by the authors and/or other copyright owners and it is a condition of accessing publications that users recognise and abide by the legal requirements associated with these rights.

- Users may download and print one copy of any publication from the public portal for the purpose of private study or research.
- You may not further distribute the material or use it for any profit-making activity or commercial gain
- You may freely distribute the URL identifying the publication in the public portal

If you believe that this document breaches copyright please contact us providing details, and we will remove access to the work immediately and investigate your claim.

Full Scale Measurements and CFD Investigations of a Wall Radiant Cooling System Integrated in Thin Concrete Walls

Tomas Mikeska, Jianhua Fan, Svend Svendsen*

Department of Civil Engineering, Technical University of Denmark, Brovej, Building 118 DK-2800 Kgs. Lyngby, Denmark

Abstract

Densely occupied spaces such as classrooms can very often have problems with overheating. It can be difficult to cool such spaces by means of a ventilation system without creating draughts and causing discomfort for occupants. The use of a wall radiant cooling system is a suitable option for spaces with a high occupant density. Radiant systems can remove most sensible heat loads resulting in a relatively small requirement for supply air for ventilation.

This paper reports on experimental and numerical investigations on a densely occupied test room equipped with a water-based wall radiant cooling system and a diffuse ceiling inlet for ventilation. A CFD model of the test room with the radiant cooling system was created. The measured temperatures and air velocities in the test room were used to validate the CFD model, which was then used for parametrical analysis.

The results show that the wall radiant cooling system based on plastic capillary tubes integrated in a thin layer of high performance concrete can provide energy for cooling between 29 W/m^2 and 59 W/m^2 of floor area with cooling water temperatures between 21.5 °C and 18.5 °C, which results in room air temperatures between 25 °C and 22 °C. The investigations elucidate the influences of the area of diffuse ceiling inlet, the cooling power of the radiant walls, the internal heat gains and the area and location of the radiant cooling walls on indoor thermal comfort and draught problems in the room. The findings in the paper would be relevant for designers, consultants and engineers when designing and dimensioning a radiant wall system with a diffuse ceiling inlet for highly occupied classrooms.

**Corresponding author: Tel.: +45-45251889, E-mail: jif@byg.dtu.dk*

1. Introduction

A highly insulated sandwich wall element made of high performance concrete is an interesting option for the façades of future low-energy buildings. Its main benefit lies in the use of a concrete with high strength in which a smaller amount of concrete material is used than in traditional concrete elements. The resulting product has a rather thin layer as the load-bearing part of a wall, which leaves more space for thermal insulation. Such a wall element has better thermal performance characteristics than conventional products. The low weight of the element is also beneficial because savings can be made on transport and manipulation on a building site. Elements made of high performance concrete are also rather environmentally friendly, because the low amount of concrete material used also means low CO_2 emissions during production.

Modern low-energy buildings need to provide good thermal performance and a good indoor environment. This is especially true for educational buildings. However, classrooms very often experience poor indoor climate, as found in various studies [1], [2], [3]. The limited supply air flow due to the risk of draught and related inability of ventilation systems to handle high internal heat gains from high-density occupation result in overheating and overall discomfort associated with “sick building syndrome” [4], [5], [6]. The cooling of densely occupied rooms using a ventilation system can also become challenging because draughts can be created due to the supply of large amounts of cold air. Furthermore, the cooling ability of a ventilation system decreases during the summer because the outdoor air is warmer. An interesting alternative to cooling with outside air is to use cold water from natural sources such as ground or sea water. The best way to make good use of the cooling potential of natural water sources is to use a system which can operate with water temperatures close to room air temperature. Use of renewable sources of energy improves the sustainability of a building and reduces its environmental impact. A radiant cooling system integrated in the inner surfaces of building structures is one promising approach. It can provide a comfortable indoor climate and at the same time improve the aesthetics and architectural value of the building because most of the technical installations are hidden in the building construction. Radiant cooling systems can handle most of the sensible heat gains, and the ventilation system need only be designed to provide the necessary air flow rates for air quality based on relevant standards [7]. Such air flow rates are usually sufficient to remove latent heat loads generated from occupants [8]. The latent heat load is the heat released from occupants by means of water vapors.

Radiant systems are optimal for small temperature differences because large surface areas are usually activated. Radiant systems can have high cooling capacity while maintaining a draught-free indoor environment, which makes them suitable for spaces with a high density of occupants such as classrooms. Limitations to the cooling capacity could include the acceptable temperature of the cooled surfaces, vertical air temperature, radiant asymmetry, or a dew-point temperature [9]. An increase of comfort in an occupied space is very often experienced when radiant heating and cooling systems are installed because they produce virtually no noise, which is very often the case for fully convective systems [9].

Occupant comfort can be achieved with higher room air temperatures when radiant systems are used for cooling purposes instead of air cooling systems. This is experienced due to a radiant heat exchange which has great impact on the operative temperature and therefore on occupant perception of the thermal environment in a room. A more uniform thermal environment is also achieved because a radiant surface will significantly influence the temperatures of surrounding surfaces in a room, including the diffuse ceiling inlet which was used as a supply diffuser for the ventilation system in this paper. As diffuse ceiling inlet, the whole area of a suspended ceiling is used as a supply diffuser. Large amounts of air can therefore be supplied into a room with rather small velocities, which decreases the risk of draught. Jacobs *et al.* carried out investigations with mechanical ventilation equipped with a diffuse ceiling inlet installed in an existing educational building. Two different types of perforated ceiling were investigated and compared with the results of a supply diffuser situated on a façade area. The results showed that the diffuse ceiling ventilation provided an indoor climate with good air quality and thermal comfort without any draught [10]. Hviid *et al.* investigated the performance of diffuse ceiling inlets installed in an office room and a classroom. Uniform air flow and temperature distribution were experienced without the creation of any draught. Various types of materials were tested as the diffuse ceiling inlet [11], [12]. A diffuse ceiling inlet with air tight connections of perforated gypsum boards was studied by Mikeska [13], resulting in an even supply of fresh air over the whole area of a suspended ceiling.

There have been a few studies dealing with applications of a radiant cooling integrated as part of a building construction. One of them includes a floor cooling installation situated in the highly glassed buildings of Bangkok airport where the floor is exposed to direct solar radiation. Simmonds *et al* describes the development and performance of the radiant cooled floor combined with displacement ventilation [14]. The authors concluded that the designed system created a

comfortable indoor climate with high thermal stratification. Most other applications of a radiant cooling involve ceiling radiant cooling panels installed in a suspended ceiling [15], [16].

This paper reports on the combined effect of wall radiant cooling and a diffuse ceiling inlet used for ventilation. The water-based radiant cooling system uses thin tubes to carry a cooling medium. The small plastic capillary tubes were cast in the inner layer of a wall element made of high performance concrete. The radiant cooling system described in this paper was designed and produced as an integrated solution and the resulting product is a fully prefabricated wall element with the radiant cooling system ready to provide the required cooling. Our literature review did not reveal any application of plastic capillary tubes cast in a layer of high performance concrete and used for radiant cooling. A simplified CFD model of a room with the radiant cooling system was developed and evaluated by results from measurements. The CFD model was then used for parametrical analysis to investigate various scenarios. This gave us a broader perspective and valuable information on the possibility of using the wall radiant cooling system combined with a diffuse ceiling inlet.

2. Methods of investigation

Performance of the wall radiant cooling system and the diffuse ceiling inlet for ventilation was studied under a steady-state situation. The main focus was on an evaluation of the indoor climate in the test room. The investigations were divided into two parts. The experimental investigations were carried out on a full scale test building specifically built for the purpose of testing prototype technical solutions. The numerical calculations were carried out by the CFD software Ansys Fluent based on a simplified CFD model of the test room with the radiant cooling system. The results from measurements were used partly as inputs for the numerical calculations and partly to assess the usability of the CFD model for further parametrical analysis.

3. Test room and measurements

3.1 The Test room

A two-floor, full scale test building situated in an outdoor environment was built to allow experimental analysis of the radiant cooling system combined with a diffuse ceiling inlet as air terminal device. The walls were built with sandwich elements consisting of two layers of high performance concrete with thermal insulation in the middle. The internal

dimensions of the test room on the 1st floor of the building were 6.05 m x 3.25 m corresponding to a floor area 19.66 m^2. The height of the test room was 2.65 m. Two airtight triple glass windows with dimensions of 2.5 m x 1.1 m were installed in the north-western wall with an overall window area of 5.5 m^2. Adjacent to the test room there was a room located on the ground floor. The floor and ceiling decks were made of hollow core concrete elements with a thickness of 0.2 m.

3.1.1 Diffuse ceiling inlet

The whole area of a suspended ceiling was made of perforated gypsum boards to create the diffuse ceiling inlet, see Figure 1. The perforations were made with holes of with a diameter of 8 mm. The perforated area was 15.5% of the total area of the suspended ceiling. The ventilation unit reduced the area of the suspended ceiling to 18.6 m^2. The test room volume was 52.9 m^3.

Figure 1: Diffuse ceiling inlet construction and connection of capillary mats to manifold pipes

3.1.2 Ventilation unit

The suspended ceiling was installed 0.25 m below the ceiling in order to separate the supply and exhaust openings of the ventilation unit, see the area marked in red in Figure 2. The supply opening with a dimension of 0.8 m x 0.1 m was situated 0.05 m below the ceiling deck. The exhaust opening with a dimension of 0.15 m x 0.1 m was on the side of the ventilation unit and situated just below the perforated suspended ceiling in the test room, see Figure 2.

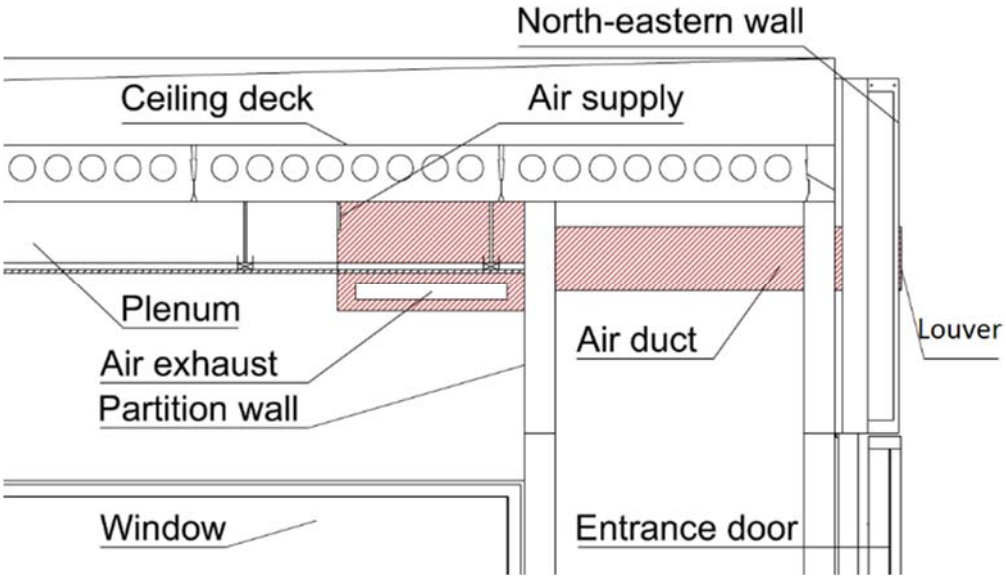

Figure 2: Ventilation unit

3.1.3 Radiant cooling system

The radiant cooling system was based on capillary mats made of polypropylene plastic capillary tubes cast in the inner layer of high performance concrete in the wall sandwich elements. The installation of the radiant systems and casting of the concrete are shown in Figure 3. Two walls were used for the radiant cooling and are shown by the blue lines in Figure 4. The walls were constructed with sandwich elements made of high performance concrete. The inner layer of concrete was 30 mm thick, the outer layer of concrete was 20 mm thick, and the thermal insulation in the middle was 300 mm thick. The special feature of the radiant system is the small diameter of the plastic capillary tubes. The outer diameter of the capillary tubes was only 4.3 mm and their wall thickness was 0.8 mm giving an inner diameter of 2.7 mm. Such a small dimension allowed the radiant cooling system to be integrated into a layer of high performance concrete only 30 mm thick. The plastic capillary tubes were connected to supply and return plastic tubes with a diameter of 12 mm, creating so-called capillary mats with a dimension of 2.7 m x 1.0 m. Altogether, there were 10 capillary mats providing a total radiant area of 27 m^2 and containing 4.32 l of cooling water in the two walls. The capillary mats were connected to the polypropylene manifold pipes by flexible hoses with an outer diameter of 10 mm. The manifold pipes had an outside diameter of 20 mm and were used to run cooling water from the technical room into the plenum, see Figure 1.

Figure 3: Casting of radiant cooling made of capillary mats

3.1.4 Investigated scenario

The investigated scenario represented a densely occupied classroom ventilated by a diffuse ceiling inlet and conditioned by a radiant wall cooling system. The 12 occupants were modeled by metal buckets with light bulbs mounted inside representing heat gains. The overall internal heat gain during the experiment was 1327 W, which was about 110 W per occupant. This included heat gains from the occupants and from equipment such as computers. The positions of the occupants, the furniture and the ventilation unit are shown in Figure 4. The mean temperature of the cooling water was 16.3 °C and the delivered cooling power was measured to be 1112 W. The cooling power of the wall was delivered with constant flow rate of cooling water and temperature. The loop with cooled water was separated from the loop situated in the walls by a heat exchanger. A regulation valve was installed in the loop with cooled water in order to maintain a constant temperature in the loop situated in the concrete walls.

The measuring point no. 3 was situated just in front of the table where the students were siting. The table was positioned close to the cooling wall. As the cold air tends to drop down, the risk of draught being created at height of ankle was considered to be high therefore the point no. 3 was chosen to evaluate it. The point 1 and the point 2 were chosen because they were in close proximity of the occupants. Additionally the point 2 was chosen with an aim to investigate the effect of the exhaust opening.

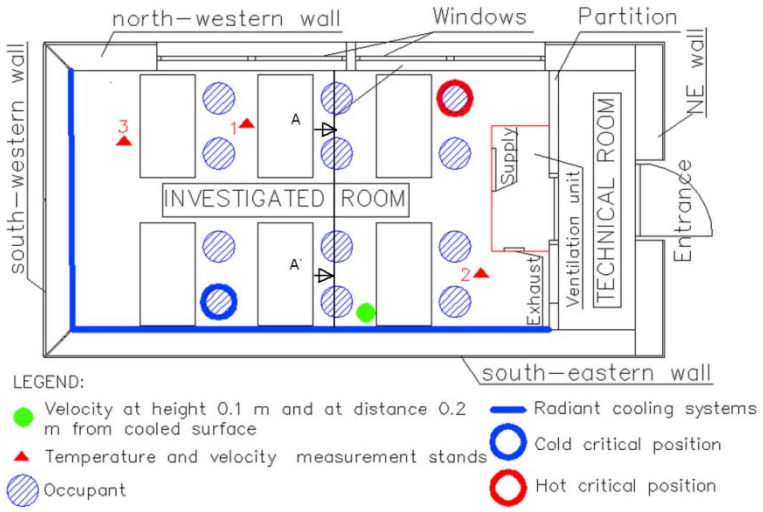

Figure 4: Horizontal view of the test room with inner/outer wall surfaces and the investigated points indicated

The temperatures were continuously measured in the test room for a period of 72 hours. The main purpose of a rather long period of measurement was to obtain measured values of temperatures and velocities in the period which are closest to a steady-state situation (a quasi-steady state). These measured values were then used in the comparisons with the results of the CFD calculations. Based on the comparison, the CFD model could be validated and used for further parametrical studies.

3.1.5 Temperature measurements

Temperatures within the test room were measured by T-type thermocouples. The acquisition units Agilent 34970A were used to process the readings. To improve the accuracy of the measurements, a reference temperature was measured at a common cold junction reference point situated outside of the Agilent's multiplexer cards. The reason for this was that the temperature difference across the whole multiplexer card can be up to 1 °C [17], which would bring an unnecessary error into the measurements. The reference temperature was measured using a thermocouple connected directly to the multiplexer card. The connection point is close to the temperature measurement point of the board. The precision of the thermocouple used to measure the reference temperature was further checked by PT100 sensors connected to a separate measuring unit. The points of interest were then measured by the thermocouples as a voltage difference and recalculated to temperatures. The precision of such a measuring setup should be about 0.3 °C [17].

Fifteen thermocouples on the three vertical stands measured room air temperatures at heights of 0.1 m, 0.6 m, 1.1 m, 1.7 m and 2.1 m as shown in Figure 4. The temperatures were measured with an interval of 1 minute. Aluminum cylinders were used to shield the thermocouples against the effects of thermal radiation. Twelve thermocouples were used to measure the wall surface temperatures. These thermocouples were attached to the walls by using a thermally conductive paste which enhanced the heat transfer between the wall surface and the thermocouples. Aluminum tape was used in this case to shield the thermocouples against thermal radiation effects. Furthermore, two thermocouples were used to measure the surface temperature of the window. Four thermocouples measured the temperature of the floor surface, and twelve thermocouples measured the surface temperatures of the diffuse ceiling inlet. In addition, air temperatures in the test room were also measured by SensoAnemo 5100F with a precision of 0.2 °C [18]. Thirty-six thermocouples were installed at three different heights in the plenum. HOBO data loggers were used to measure the outside air temperature with an accuracy of 0.35 °C [19].

3.1.6 Velocity measurements

Transducers SensoAnemo 5100SF with an accuracy ±0.02 m/s ±1% of a reading were used to measure air velocities below 5 m/s in the test room [18]. The measurements took place on the three vertical stands as shown in Figure 4, at heights of 0.1 m, 1.1 m and 1.7 m. Draught rating was used to relate draught magnitude to indoor environment comfort, including the effects of both velocities and temperatures. The recommended standard is to keep the draught rating value below 15% [20]. The maximum velocity in the occupied zone should not exceed 0.19 m/s in a cooling scenario for class B [20]. The draught rating was calculated according to Eq.(1):

$$DR = (34 - t_a) \cdot (v - 0.05)^{0,62}(0.37 \cdot v \cdot T_u + 3.14) \qquad \text{Eq.(1)}$$

where: t_a is the air temperature at the place of measurement [$^{\circ}C$], v is the mean air velocity at the place of measurement [m/s], and T_u is the turbulence intensity at the place of measurement [%]. The turbulence intensity is defined as the ratio of the root-mean-square of the turbulent velocity fluctuations and the mean velocity.

3.2 Numerical simulations

The aim of the development of a CFD model of the test room with the radiant cooling system was to allow for deeper understanding of the system and to facilitate efficient and economical optimization of its design, taking into account

various parameters. The developed CFD model is depicted in Figure 5. The commercial CFD program Ansys Fluent 14.0 was used in the numerical simulations [21].

3.2.1 The grid creation

A hexahedral grid was created by using a sweep method. The grid was refined in the areas close to the wall surfaces to allow for correct calculation of heat transfer. The maximum skewness of the model was 0.3 and the average value was less than 0.00045. The mesh had 4,354,482 cells. The grid independence was investigated and the results were published [22].

3.2.2 Boundary conditions

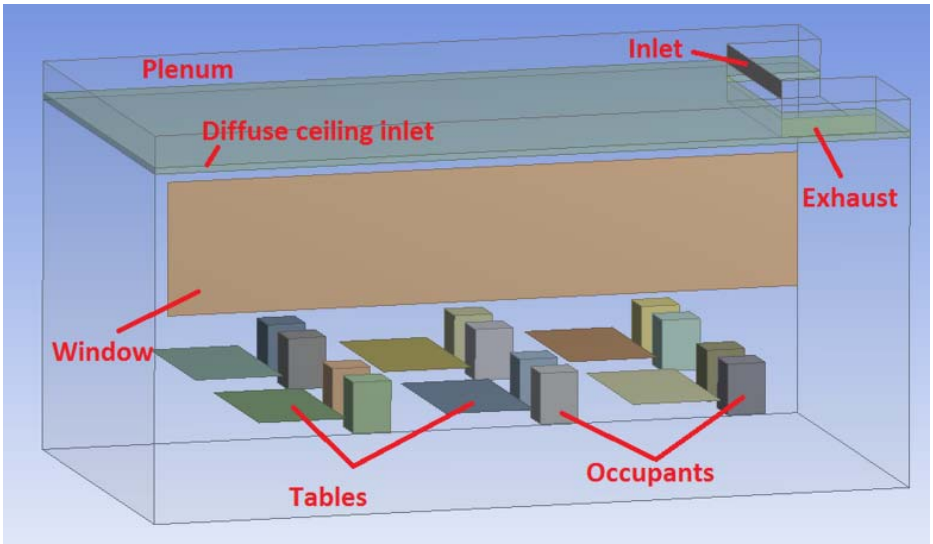

Figure 5: CFD model

The boundaries in the CFD model are depicted in Figure 5. The inlet boundary, with a dimension of 0.8 m x 0.1 m, was assigned a velocity magnitude of 1.44 m/s and a temperature of 26.6 °C, as measured in the experiment. The ventilation flow rate was 115 l/s, which was determined in order to fulfill the requirement of indoor air quality according to the standards [7]. The exhaust element, with a dimension of 0.45 m x 0.10 m, was defined as a pressure outlet with an exterior pressure of 0 Pa. The rectangular blocks, with a dimension of 0.25 m x 0.20 m and a height of 0.45 m, were used to model the seated occupants and were placed on horizontal plates at a height of 0.55 m. The tables were modeled as horizontal plates with a dimension of 1.3 m x 0.7 m and placed at a height 0.7 m. The wall surfaces of the room were defined as nonslip walls with external heat transfer coefficients of 0.18 W/(m^2·K) for the roof, 0.19 W/(m^2·K) for the walls, 2.47 W/(m^2·K) for the floor, and 1.26 W/(m^2·K) for the windows, as determined by the experiment. A measured

surrounding air temperature of 8.5 °C was used as free stream temperature for the roof, the walls and the windows while the floor was assigned a free stream temperature of 19.8 °C, which was the air temperature measured in the room below the floor. The solar radiation from the window was not modeled because the measurements used to validate the CFD model were taken in a period where no direct sunlight was present.

3.2.3 Porous zone model

The porous gypsum panels creating the diffuse ceiling inlet were modeled by using a porous zone model in Ansys Fluent. The porous zone model in Fluent is defined as a fluid domain with an added momentum loss equation. The inputs to the model were determined based on the measured pressure drop across the suspended ceiling. The porosity was set as isotropic with a value of 15.5%, in accordance with the known open area of the perforated gypsum plate. The momentum loss was defined by the viscous (1/a) and inertial resistance coefficients C_2. These values were obtained by quadratic regression analysis of the measured values of the pressure drop and the velocity, shown in Eq. (2):

$$\Delta p = C_2 \cdot \frac{1}{2}\rho \cdot \Delta n \cdot v^2 + \frac{\mu}{a} \cdot \Delta n \cdot v \qquad \text{Eq. (2)}$$

where: Δp is the pressure drop measured across the porous suspended ceiling in Pa and v is the velocity of the air flowing through porous suspended ceiling in m/s. ρ is air density, kg/m^3. Δn is thickness of the gypsum panels, m. μ is air viscosity, kg/(ms). C_2 is the inertial resistance factor which was determined by the experiment to be 1,185,000 m^{-1}. 1/a is the viscous resistance coefficient, which was found to be 1.306x10^9 m^{-2}.

3.2.4 Turbulence modeling and near wall treatment

It was important to consider buoyancy forces in the CFD model because they influence air movement in rooms equipped with a diffuse ceiling inlet to a considerable degree. A Boussinesq model was used to account the buoyancy forces. The reference temperature was defined as the average temperature in the calculated domain. The investigations were carried out as steady-state calculations. The semi-empirical, two-equation k-ξ model was used to model the turbulent effects in the test room. The model is normally used for fully developed turbulent flows and is therefore suitable for free stream areas of a domain [23]. The RNG k-ξ model was used because it partly accounts for low Reynolds number effects when combined with optimal near wall treatment [24]. However, the k-ξ turbulence model has its limitations in close-to-the-wall regions, and it very often yields high wall shear stress and high heat transfer rates [23]. That is why the k-ξ turbulent model needed to be combined with proper near wall treatment. The scalable wall function was applied

to resolve the area close to the surfaces in the test room. The scalable wall function has the advantage over other types of wall functions because there is no limitation on the grid spacing close to the wall surface. The limiting value of 11.067 was used to ensure that the first grid point would always be in the logarithmic profile area [23].

4. Results and discussion

4.1 Temperatures

Figure 6 shows the results of the temperatures measured in the test room over a period of 72 hours. The blue interval indicated by blue lines with arrows in the figure represents time of the day from 8AM to 5PM. In the experiment there was a constant heat gain from occupants. The aim was to identify the most stable period in terms of operative temperature which was then used for validation of the CFD model**.** The three most stable periods were found each day in the early mornings between 4 a.m. and 7 a.m., as shown by the horizontal red lines with arrows. The measurements of the last of these periods were used for the validation of the CFD model (farthest right in Figure 6). The temperatures and velocities in the test room were measured at the same time. The last period was considered to be in a quasi-steady-state situation because the temperatures did not change markedly. The outside temperature was also rather stable during that period. It can be seen that temperatures in the test room were generally rather low during our measurements. There were two critical positions in the occupied space where occupants could feel thermal discomfort. The first position was close to the two cooling wall, where the occupant might feel too cold as shown by the blue circle in Figure 4. The second position was in the opposite corner of the test room, where the occupant might feel too hot as shown by the red circle in Figure 4, because this position was farthest from the cooled surfaces. The operative temperatures at the two critical points were close to 23 °C and 22 °C for the hot and the cold critical points, respectively, representing environment category classes B and C, respectively [7]. As the main purpose of the measurement was to get reliable data which could be used for validation of the CFD model, the experiment was not especially controlled to achieve a better indoor environmental category. As can be seen from Figure 6, the influence of the radiant cooling systems on the operative temperature in the test room was rather significant. The average temperature of the cooled surfaces was 18.8 °C. Regular small fluctuations in the inlet air temperature were observed as a result of the ON/OFF operation of the electrical heater in the ventilation unit. The irregular larger fluctuations were a result of the algorithm used by the control system of the ventilation unit, which could not be changed.

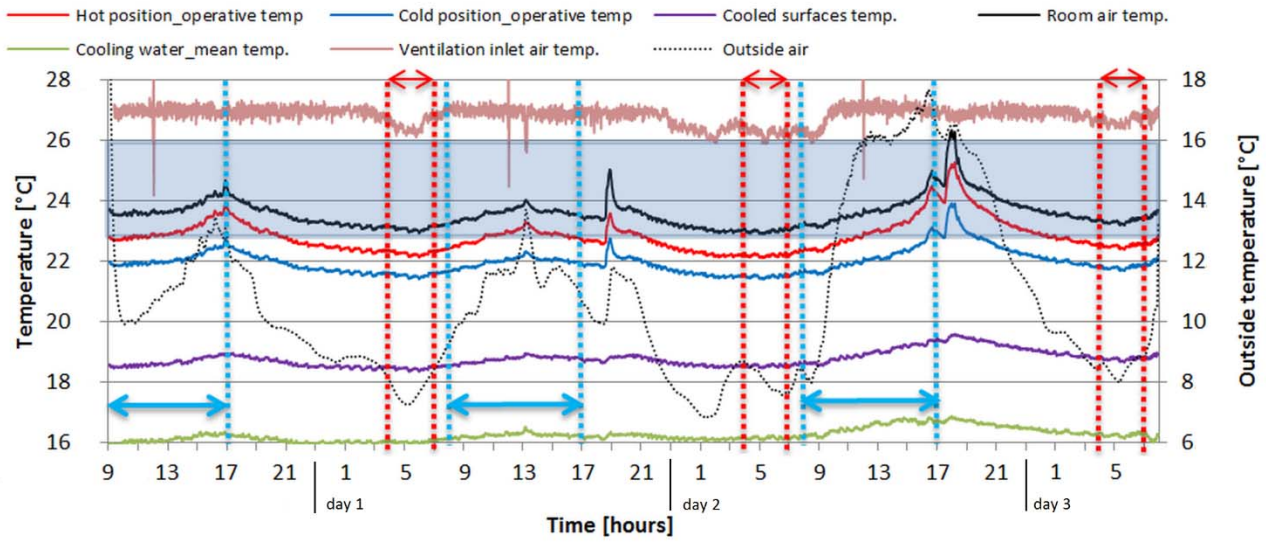

Figure 6: Temperature development from measurement

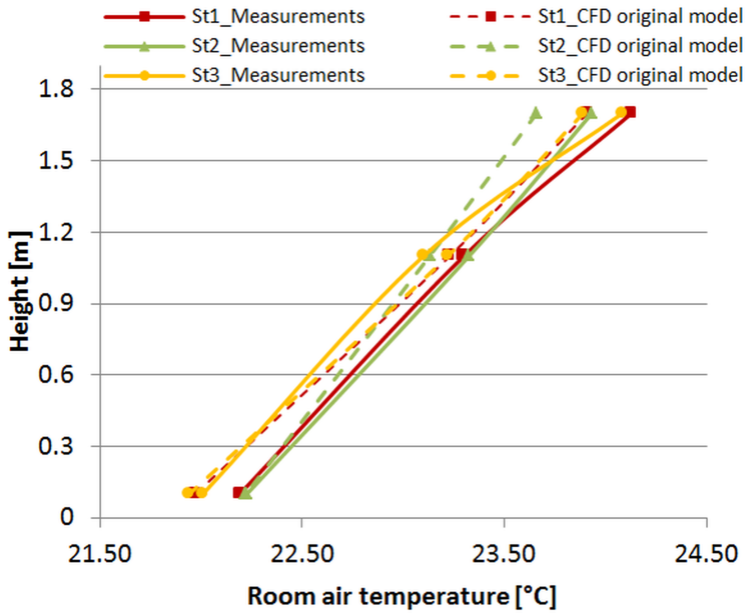

Figure 7: Measured and CFD temperature distribution in the room

Figure 7 shows the measured and the CFD calculated air temperatures in the test room in the quasi-steady-state period. The measured vertical temperature difference between the lowest (0.1 m) and the highest (1.7 m) measurement points was 2 K, which is within environmental class A [20]. As can be seen from Figure 7, the room air temperatures calculated by the CFD model were in good agreement with the measured values. The maximum temperature difference between the measurements and the CFD predictions was 0.3 K. In general, the calculated temperatures were slightly lower than the measured values at all heights. The vertical temperature difference obtained from CFD calculations was also

consistent with the measurements. A cold draught close to the cold surfaces could create a large vertical temperature difference in the test room, and it is therefore very important that the CFD model was able to capture this behavior.

4.2 Air velocities

As can be seen from Figure 8, the room air speeds were generally slightly higher in the lower part of the test room as a result of buoyancy forces induced by the internal heat sources and the vertical walls activated for cooling. It is difficult to obtain good velocity predictions by means of CFD calculations due to the complexity of velocity prediction and due to the simplification of the test room in the CFD model, for instance, legs of chairs and tables, small obstacles on the floor etc. As can be seen from Figure 8, the CFD calculation slightly underestimated the air velocities in the test room. However, the air speed within the test room was generally very low and therefore the differences were actually minor. The limiting value 0.24 m/s according to ISO 7730 [20] was never reached in the CFD calculation, which is in good agreement with the measurement. The draught rating is evaluated to be all zero for the three stands by the CFD model, while the measurement shows a draught rating of zero for the stands as well except a rating of 5.1% for the stand 2 at a height of 0.1 m. Although there were minor differences (max. 0.04 m/s) between the CFD calculated and the measured air speeds, the differences will not change the conclusion on comfort category, therefore the evaluation of indoor comfort category by the CFD model is correct. In conclusion, the CFD model was considered reliable for the investigated case, thus can be used for the subsequent parametrical analysis. The main benefit of CFD velocity predictions is to identify places with potentially high risk of draught. The room air cooled by the cold surfaces moved down towards the floor, as can be seen in Figure 9. This could potentially result in the creation of cold draughts at the height of ankles as result of the acceleration of cold air. However, this did not happen because the velocities measured close to the cold walls were higher at heights of 1.1 m and 1.7 m than at the height of 0.1 m, as can be seen in Table . This can be explained by good mixing of the air in the room as a result of the interaction of the thermal plums created by the heat sources situated in the room and the colder incoming air. The downward air flow was located at a height of 1.1 m, partly directed to the center of the test room, as can be seen in Figure 9. In conclusion, the heat sources situated in close proximity to the cooled surfaces could have had a high influence on the flow pattern close to the cooled walls. The CFD calculation shows the area in the test room where the down draughts from the two cooled walls collided. It is the place where the air velocity increased and a unique diagonal flow pattern was created across the test room. The result at height 0.1 m

is shown in Figure 20 (farthest left). Because the measuring stands were situated in different positions in the test room during our measurements, this diagonal flow pattern was not captured in the measurement.

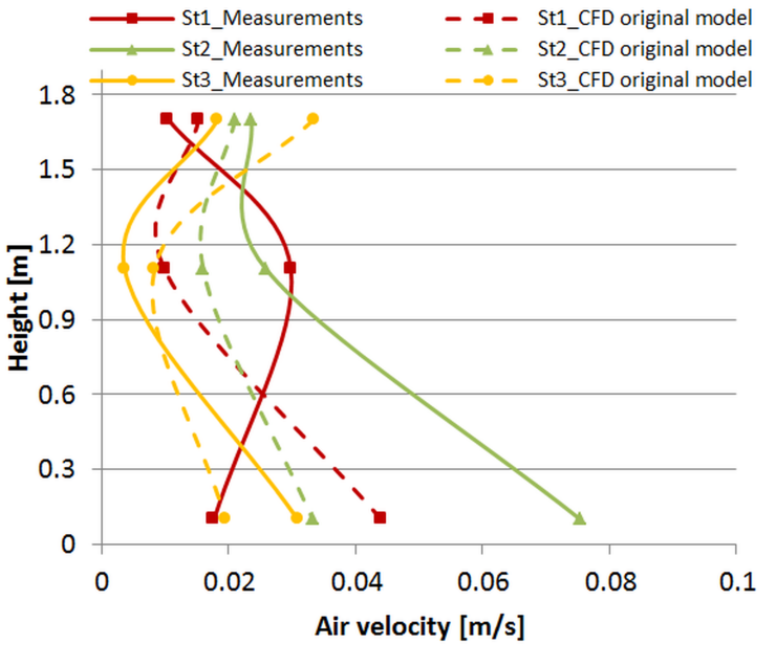

Figure 8: Measured and CFD velocity magnitude distribution in the room

Table 1: Measured velocity magnitude close to the south-eastern wall in m/s

Distance from wall	Height		
[m]	1.7[m]	1.1[m]	0.1[m]
0.2	0.11	0.15	0.09
0.05	0.31	0.25	0.15
0.01	0.33	0.28	0.15

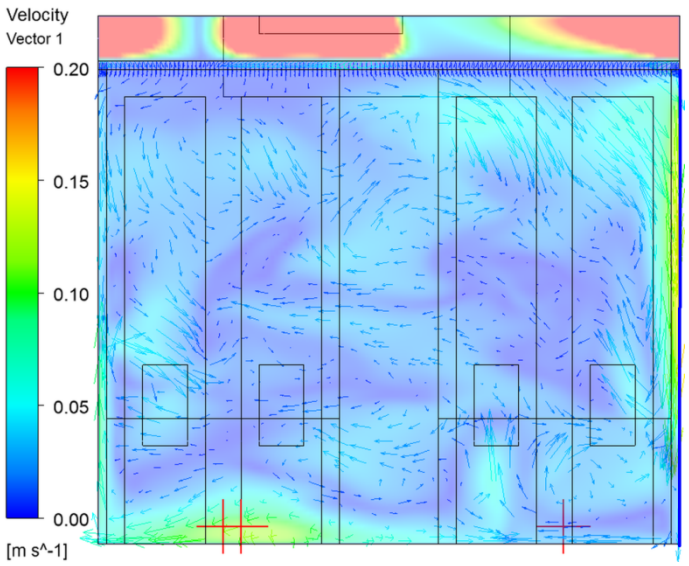

Figure 9: Velocity distribution in the transverse plane A-A´ as shown in Figure 4 (cooling walls marked in blue)

It should be noted that the experiment was carried out continuously with a constant heat load from occupants and that the focus of the paper is on steady state condition of the room during occupied hours. Although the CFD model was validated by measurement between 4 AM and 7 AM, it still can represent teaching hours. The thermal conditions in the room out of the teaching hours are not the interest of the paper. Since the material properties, boundary conditions and the governing equations used in the CFD model are valid for a much wider temperature range and the temperature difference between these different scenarios is just a few degrees, the CFD model can also be used to calculate other situations outside of the validated temperatures.

4.3 Parametrical analyses

4.3.1 Reduced area of diffuse ceiling inlet

To investigate the effect of a different suspended ceiling setup on the indoor climate of the investigated test room, a scenario with a reduced area of the diffuse ceiling inlet was studied using the original CFD model. The area of the diffuse ceiling inlet was reduced to the area of three rectangles situated above the tables. The new supply area is shown in green in Figure 10. Each supply rectangle had a dimension of 3.15 m x 0.70 m, giving an overall area of 6.60 m² and corresponding to 35% of the original supply area. The rest of the suspended ceiling was assumed to be covered by solid

gypsum through which air could not penetrate – shown in red in Figure 10. The settings of the ventilation and cooling system were kept the same as in the original model.

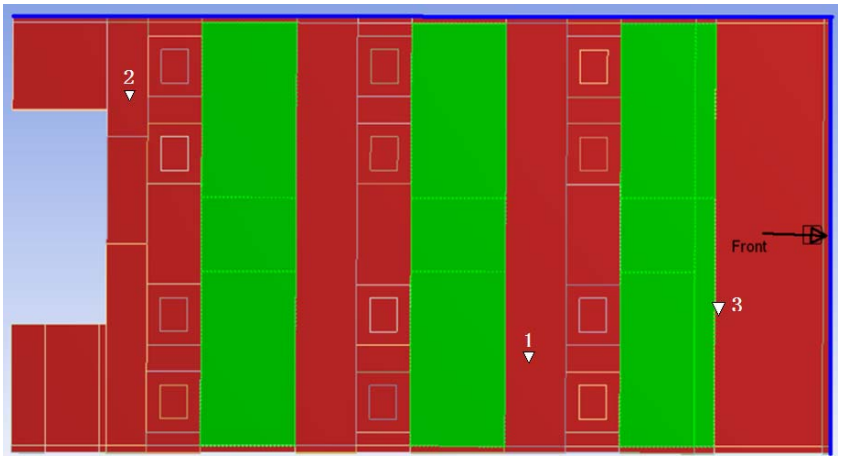

Figure 10: Layout of scenario with reduced area of diffuse ceiling inlet (cooling walls marked in blue)

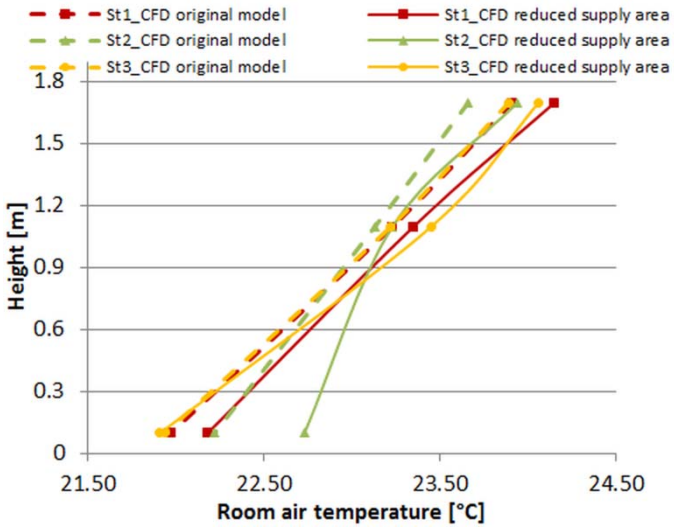

Figure 11: Temperature distribution in scenario with reduced supply area

Figure 11 shows comparison of the temperature distribution between the scenario with a reduced supply area and the original scenario. The temperature of the cooled surfaces was 18.5 °C. The temperature development in the test room was very similar for both scenarios except for the situation on stand 2. A disruption in the general flow pattern occurred in this area, as can also be seen from the velocity development shown in Figure 12.

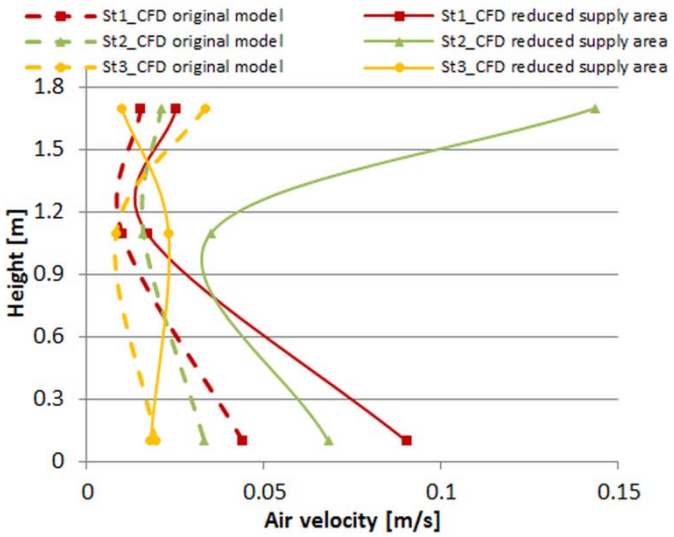

Figure 12: Velocity development in scenario with reduced supply area

The results show that reducing the area of the diffuse ceiling inlet by a factor of 3 did not pose any limitations in terms of temperature and velocity distributions in the test room, because the differences in these calculations were rather small. This is an important finding since in practice it is not always possible to utilize the whole area of the ceiling for ventilation.

4.3.2 Various temperatures of cooled surfaces

The temperature distribution within the test room for the original scenario and the scenario with reduced supply area are shown in Figure 13 for different wall temperatures. The purpose of the investigations was to find out the effect of various cooled wall temperatures on the temperature and velocity distribution in the test room and on the risk of draught creation. The results are shown for three different cooled surface temperatures: 14 °C, 18.5 °C and 21.5 °C. These temperatures correspond to a power output from the cooled walls of 1200 W, 780 W and 500 W, respectively. The temperature distribution pattern was similar for both scenarios, confirming the previous conclusion that reducing the supply area did not make much difference to the temperature distribution within the test room. This applies to all three cooled surface temperatures investigated. The vertical temperature difference was slightly higher when the temperature of the cooled surfaces was decreased to 14 °C. The explanation is that when the temperature of the cooled walls was low, higher velocity was experienced close to the cooled surfaces and higher volumes of cold air were distributed to lower parts of the test room. The velocity at a height of 0.1 m and at a distance of 0.01 m from the south-

eastern wall was 0.05 m/s, 0.04 m/s and 0.03 m/s for the cooled surface temperature of 14 °C, 18.5 °C and 21.5 °C, respectively.

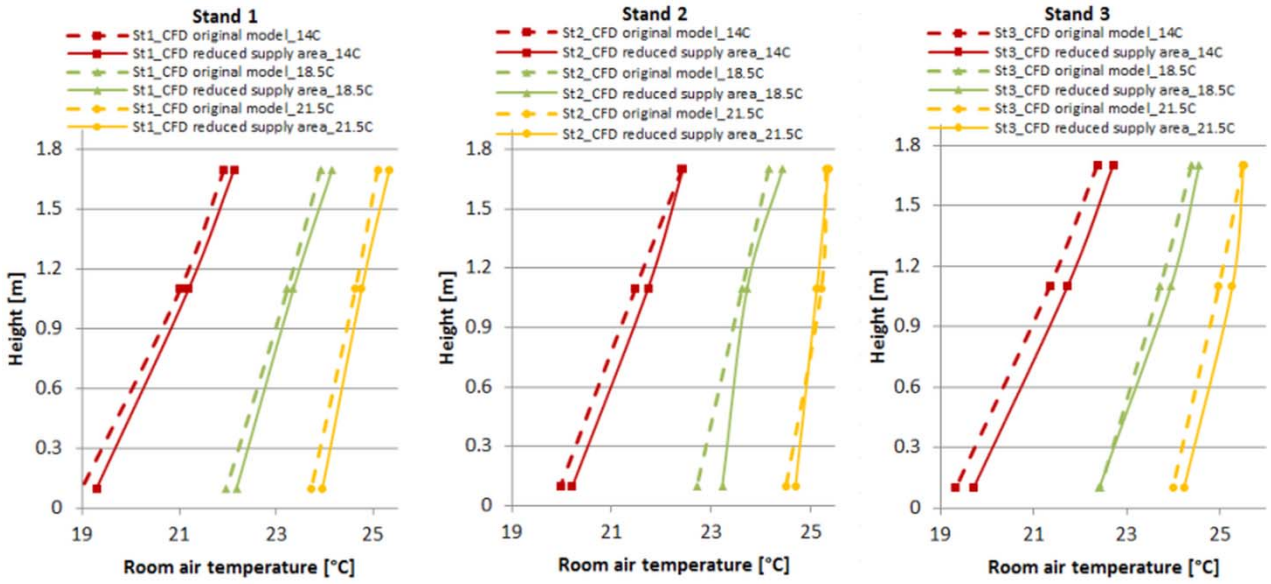

Figure 13: Comparison of temperature distribution between the original scenario and the scenario with reduced supply area with various wall temperatures

Figure 14 shows the results of the velocity distribution for the original scenario and the scenario with reduced supply area with a cooled surface temperature of 14 °C, 18.5 °C and 21.5 °C, respectively. The velocity distribution within the test room is very similar in both scenarios except on stand 2. The velocity increased in both CFD models at a height of 0.1 m when the cooled wall temperature was 21.5 °C. The reason can be seen in Figure 15, where a flow pattern with higher velocity was created in the corner of the test room (the upper right-hand corner in Figure 15). A concrete explanation of this phenomenon, however, is not known. A similar flow pattern can be seen when the cooled surface temperature was 14 °C. It could be argued that it was a result of the low temperature of the cooled wall surface. Despite this phenomenon, the critical velocities which would result in draught problems were not exceeded in any of the investigated scenarios.

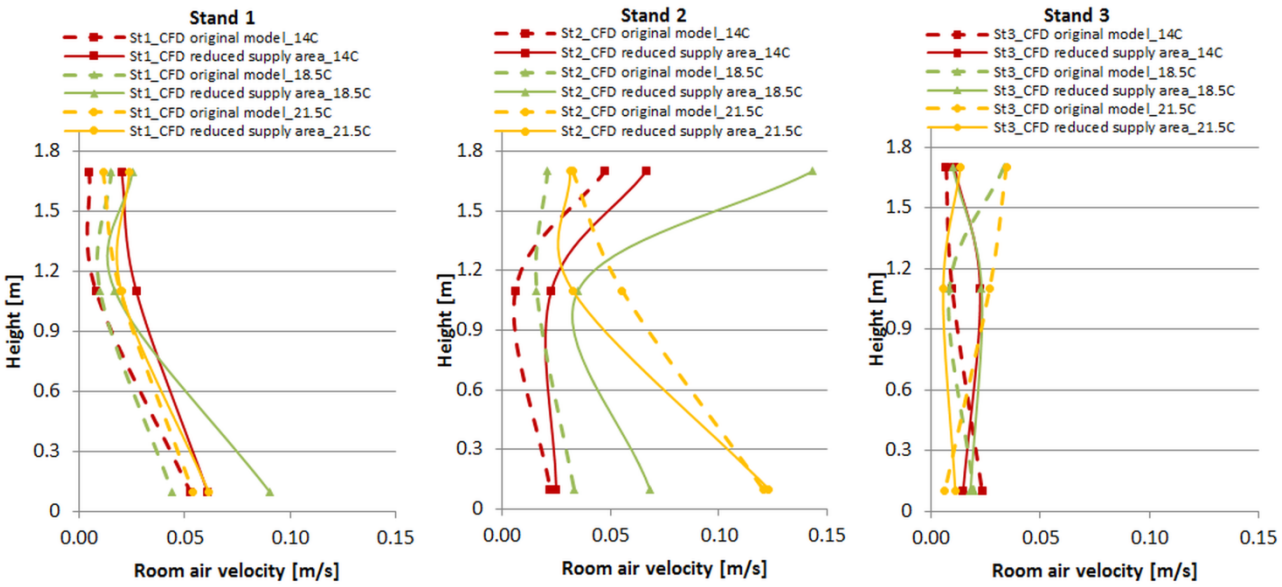

Figure 14: Comparison of velocity magnitude distribution between the original scenario and the scenario with reduced supply area with various wall temperatures

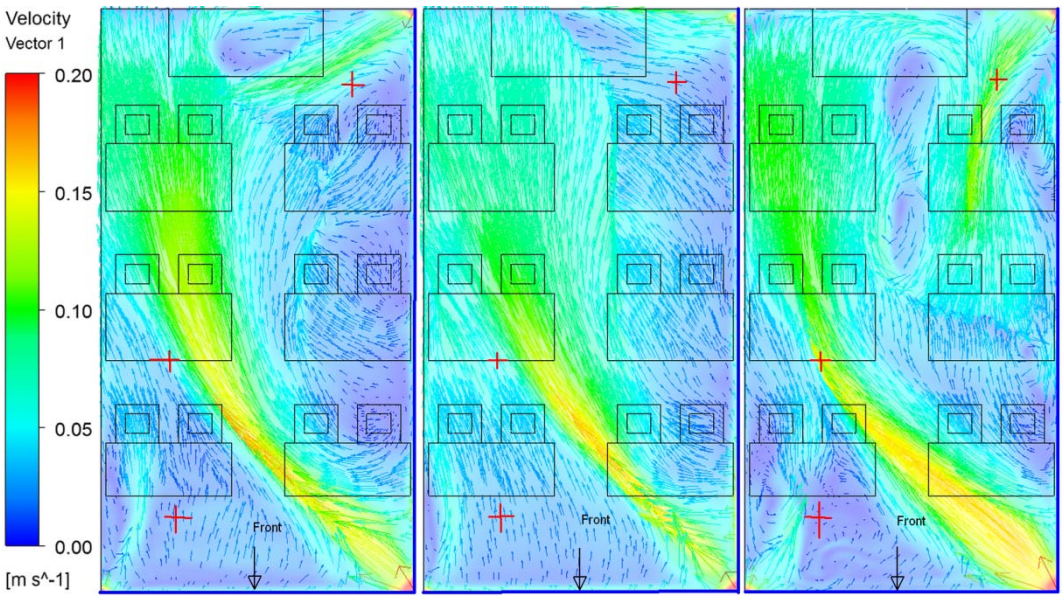

Figure 15: Velocity distribution in the horizontal plane at a height of 0.1 m: 14 °C (left); 18.5 °C (middle); 21.5 °C (right) (cooling walls marked in blue)

4.3.3 Heat gains variation

Figure 16 shows the air temperatures in scenarios with different internal heat loads. The original scenario had an internal heat gain of 1327 W. Two more scenarios were investigated: one with a decreased heat load of 664 W and one with an increased heat load of 2654 W. It can be seen in Figure 16 that the vertical temperature difference was increased with a decrease of the internal heat loads.

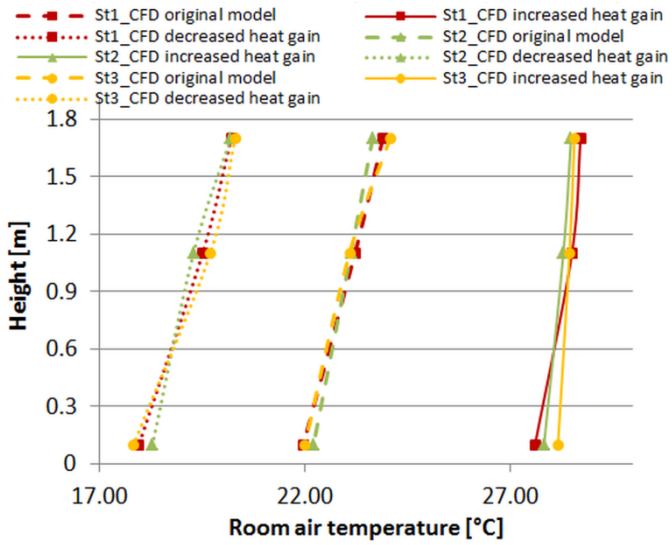

Figure 16: Temperature distribution in scenarios with different heat loads

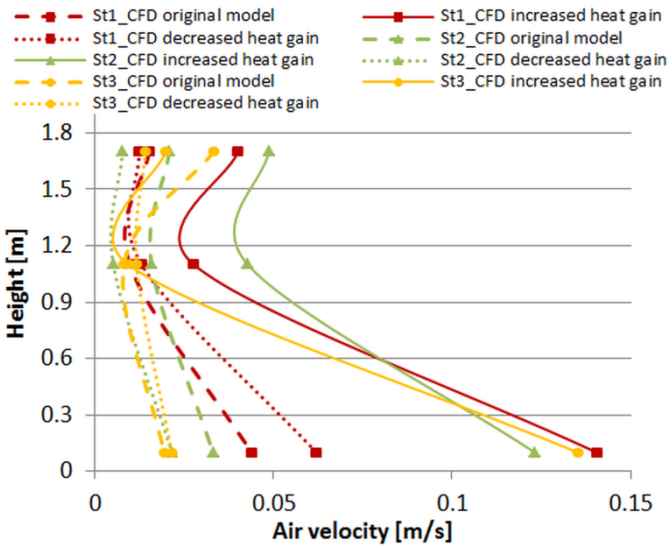

Figure 17: Velocity distribution in scenario with increased and decreased heat load

The velocity distribution in the test room for the scenarios with different internal heat loads is shown in Figure 17. Increased internal heat loads resulted in higher velocities throughout the whole test room, especially in areas close to

the floor. The results support the finding that air flows in the test room were significantly influenced by buoyancy forces. The results of draught ratings for the scenarios with various internal heat loads are shown in Table . It is shown that with an increase of the heat load there is an increased risk of draught in the room at a height of 0.1 m.

Table 2: Draught ratings (in %) for scenarios with increased and decreased internal heat loads

Height	CFD original model			CFD increased heat loads			CFD decreased heat loads		
[m]	St1	St2	St3	St1	St2	St3	St1	St2	St3
0.1	0.0	0.0	0.0	4.6	6.1	4.0	3.3	0.0	0.0
1.1	0.0	0.0	0.0	0.0	0.0	0.0	0.0	0.0	0.0
1.7	0.0	0.0	0.0	0.0	0.0	0.0	0.0	0.0	0.0

4.3.4 One wall used for cooling

The purpose of this investigation was to find out the effect of activating only one wall for cooling instead of two walls as in the original scenario. Two scenarios were investigated, where in the first scenario only the south-eastern wall was activated and in the second scenario only the south-western wall was activated for cooling. The same cooling power as in the original scenario was used for both new scenarios to make them comparable.

The surface area of the cooled wall was different in each scenario, so the temperature of the cooled surfaces also differed. The cooled surface temperature was 18.8 °C in the original scenario, 17.8 °C in the scenario with the south-eastern wall, and 12.3 °C in the scenario with the south-western wall.

Figure 18 shows the temperature distribution in the test room for the scenarios with different surfaces activated for cooling. The temperature development is similar for all scenarios except for the situation on stand 1 at a height of 0.1 m, which was caused by strong flow patterns created along sides of the test room as can be seen in the right-hand picture in Figure 20. The stands are shown by the red crosses in Figure 20 and the positions of the measuring stands are depicted in Figure 4. The vertical temperature differences were slightly higher at all stands for the scenario with the south-western wall activated for cooling.

Different behavior was observed in the case of velocity development. As can be seen from Figure 19, higher velocity was observed on stand 3 at a height of 0.1 m in the scenario with the south-western wall activated for cooling. This was because the low temperature of the south-western wall created a down draught. The increased velocity in the plane

0.1 m above the floor can be seen in Figure 20, which shows the velocity distribution in the room at a height of 0.1 m for the three scenarios.

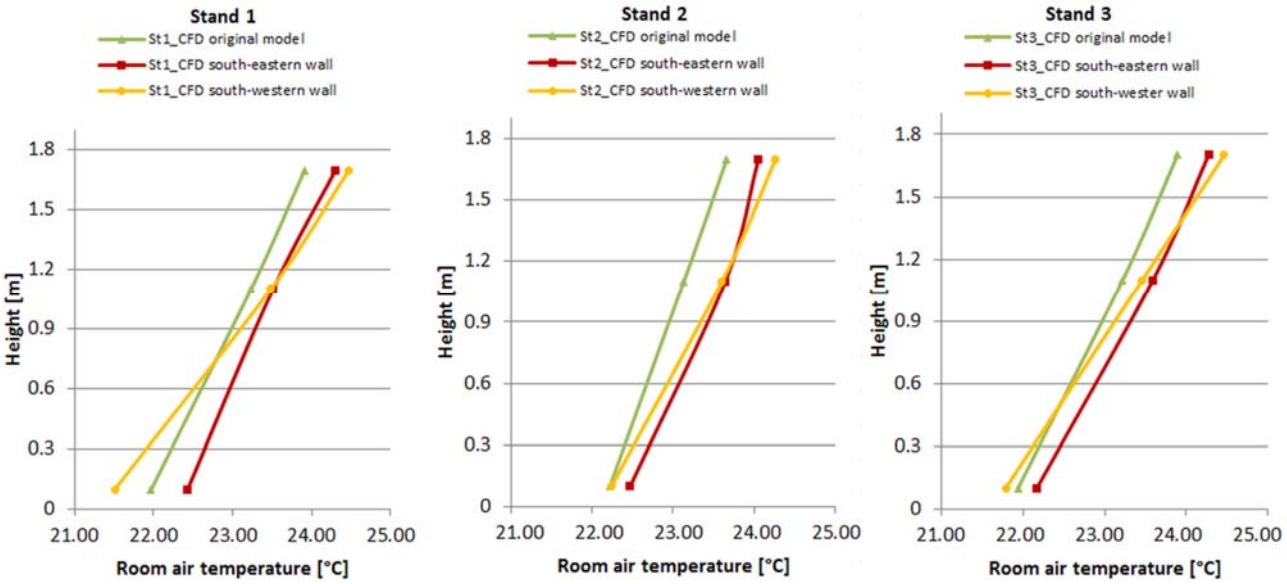

Figure 18: Temperature distribution in scenarios with different surfaces activated for cooling

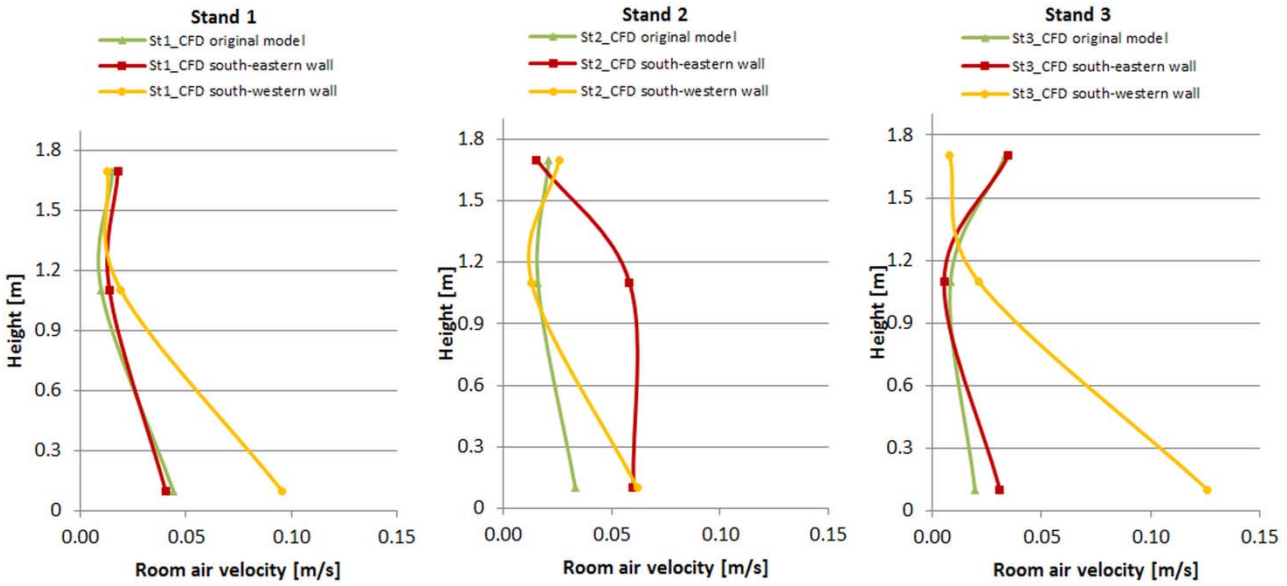

Figure 19: Velocity distribution for scenarios with different surfaces activated for cooling

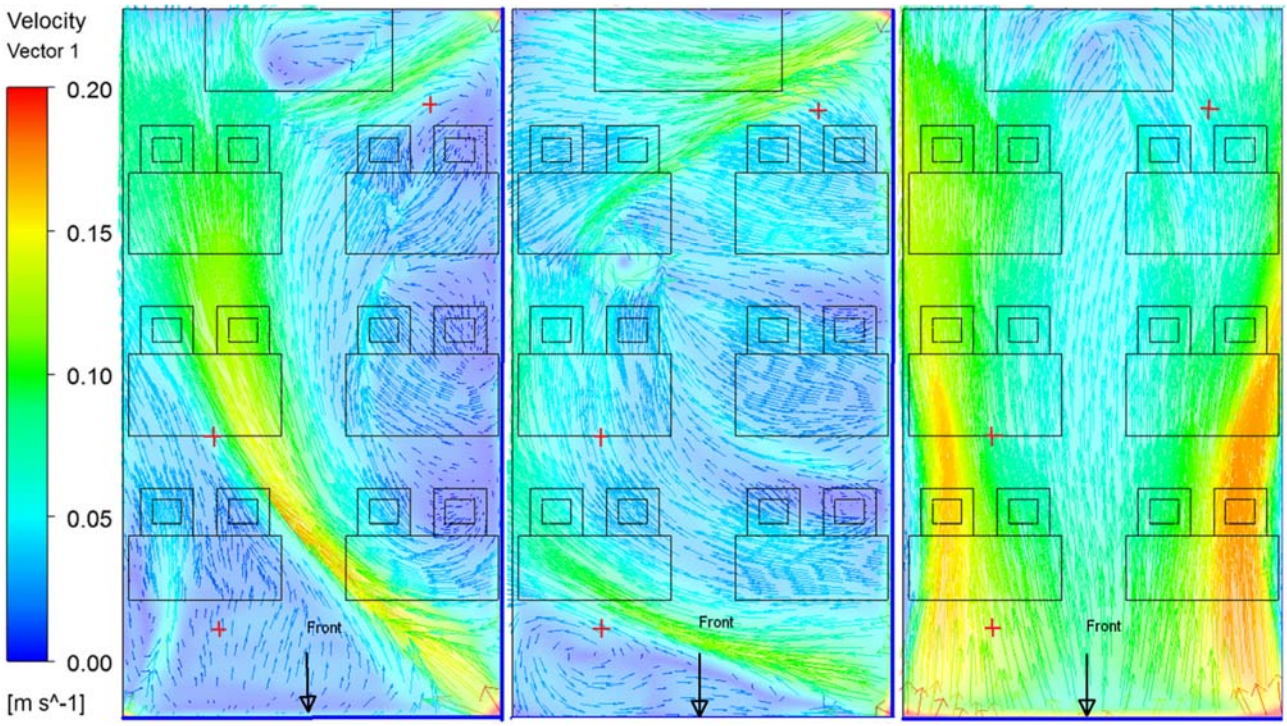

Figure 20: Velocity distribution at height 0.1m for three scenarios: original model (left); south-eastern wall (middle); south-western wall (right) (cooling walls marked in blue)

Rather a strong flow pattern is observed diagonally through the test room when both walls were activated for cooling, as can be seen in the left-hand picture in Figure 20. This flow pattern is in the area where the down flow from the south-eastern wall collides with the down flow from the south-western wall, resulting in higher velocity. When only the south-eastern wall is activated for cooling, the flow pattern is not so strong and is situated in a slightly different position in the test room. The recirculated area is in the corner of the test room, as can be seen in the bottom left-hand corner of the middle picture in Figure 20. The activation of only the south-western wall for cooling creates strong flow patterns along the sides of the long walls, as can be seen in the right-hand picture in Figure 20.

The draught ratings for all scenarios are shown in Table 3. As the above investigations have already indicated, the highest draught ratings were found in the scenario with the south-western wall activated for cooling.

Table 3: Draught ratings (in %) for scenarios with different walls activated for cooling

Height	CFD original model			CFD south-eastern wall activated			CFD south-western wall activated		
[m]	St1	St2	St3	St1	St2	St3	St1	St2	St3
0.1	0.0	0.0	0.0	0.0	2.7	0.0	5.8	3.0	7.8

1.1	0.0	0.0	0.0	0.0	2.1	0.0	0.0	0.0	0.0
1.7	0.0	0.0	0.0	0.0	0.0	0.0	0.0	0.0	0.0

4.4 Analysis and discussions

By means of the parametric study using the CFD models, the suitability of a wall radiant cooling system with a diffuse ceiling inlet for ventilation of a highly occupied classroom is evaluated in terms of thermal comfort and draught problem. The analysis shows that this concept of ventilation for classrooms offers flexibility for design of the diffuse ceiling inlet. The system can be used for rooms with different diffuse ceiling inlet areas (corresponding to a coverage ratio between 35% and 100%) without creating any draught problems. A cooled surface temperature of 14 °C, 18.5 °C and 21.5 °C was investigated, corresponding to a cooling capacity of 1200 W, 780 W and 500 W respectively for the 27 m^2 cooling wall. The results show that with an increase of the cooling capacity the risk of draught in the room is increased, which can be explained by the stronger buoyancy forces with increased cooling capacity of the wall, creating large downward air flow in the corner between the two cooling walls. However within the cooling capacities investigated in the paper there is no sign of significant draught risk in the room. An investigation of the heat loads shows that with an increase of the heat load in the room there is an increase of air speed in the room throughout the room, indicating that there might be a risk of draught for a heat load higher than 2654 W. The influence of the area of cooling wall surface on the performance of the wall radiant system was investigated. The results show that with a decrease of the active wall radiant surface area there is an increase of draught risk due to the fact that the cooling capacity of the wall in W/m^2 increases significantly with the decrease of active radiant wall surface area. For better indoor thermal comfort it is better to have more walls activated for cooling.

The wall radiant cooling system combined with a diffuse ceiling inlet for ventilation created a comfortable indoor climate in a classroom with a high density of occupants of 0.6 per m^2 of floor area. The radiant system provided energy for cooling between 29 W/m^2 and 59 W/m^2 of floor area with cooling water temperatures of between 21.5 °C and 18.5 °C. The resulting indoor air temperature was between 25 °C and 22 °C. The value 29 W/m^2 can be assumed as a suitable and sufficient amount of cooling power for the scenarios investigated in the test room with a ratio of cooling walls to floor area of 1.2. This means that a low temperature difference between cooling water and room air of 4.5 K is sufficient to maintain a comfortable indoor climate. This is favorable for the use of renewable sources of cooling water, such as ground water and sea water. The highest measured draught rating of 5.1% was experienced in the area close to the

floor, so the system did not create draught. Our measurements showed that the radiant cooling system had a rather high influence on the operative temperature, which was as much as 2 K lower than the room air temperature.

These findings would be relevant for designers, consultants and engineers when designing and dimensioning a radiant wall system with a diffuse ceiling inlet for highly occupied classrooms.

5. Conclusion

Experiments were carried out on a full scale test room under outdoor conditions in order to evaluate performance of a wall radiant cooling system combined with a diffuse ceiling inlet for ventilation. A simplified CFD model of the test room with the radiant cooling system was developed and evaluated by results from measurements. It is shown that the CFD model predicted well the air temperatures in the room. Although there were minor differences between the CFD calculated and the measured air speeds in the room, the evaluation of the indoor comfort category by the CFD model was considered satisfactory.

The CFD model was used for parametrical analysis to investigate the influence of the area of diffuse ceiling inlet, the cooling power of the radiant walls, the internal heat gains and the area and location of the radiant cooling walls on indoor thermal comfort and draught problems in the room. The results show that this concept of ventilation for classrooms offers flexibility for design of the diffuse ceiling inlet. The system can be used for rooms with different diffuse ceiling inlet areas (corresponding to a coverage ratio between 35% and 100%) without creating any draught problems. Higher internal heat gains in the room and higher cooling power of the walls will result in higher velocities especially in areas close to the floor, increasing the risk of draught problem in the room. This suggests that the air flows in the test room were governed to a considerable degree by buoyancy forces. A low temperature difference between the cooling water and the room air of 4.5 K is sufficient to maintain a comfortable indoor climate. This is favorable for the use of renewable sources of cooling water, such as ground water and sea water.

These findings would be relevant for designers, consultants and engineers when designing and dimensioning a radiant wall system with a diffuse ceiling inlet for highly occupied classrooms.

Acknowledgement

This research came to existence thanks to kind sponsorship of companies Airmaster®, Knauf Danoline®, and Connovate A/S. We were able to do thorough numerical investigations thanks to the cooperation initiated by the Sino-Danish Center for Education and Research and the high performance computing platform kindly provided by the Beijing Computing Center.

Bibliography

[1] P. Wargocki and D. P. Wyon, "Providing Better Thermal and Air Quality Conditions in School Classrooms Would Be Cost-effective," *Building and Environment,* vol. 59, pp. 581-589, 2013.

[2] D. G. Shendell, W. J. Fisk, M. G. Apte, D. Faulkner, R. Prill and D. Blake, "Associations Between Classroom CO2 Concentrations and Student Attendance in Washington and Idaho," *Indoor Air,* no. LBNL-54413, 2004.

[3] M. Turunen , O. Toyinbo, T. Putus, A. Nevalainen, R. Shaughnessy and U. Haverinen-Shaughnessy, "Indoor Environmental Quality in School Buildings, and the Health and Wellbeing of Students," *Int. J. Hyg.Environ.Health,* 2014.

[4] D. Clements-Croome, "Work Performance, Productivity and Indoor Air," vol. SJWEH Suppl (4), pp. 69-78, 2008.

[5] H. Levin, "Sick Building Syndrome: Review and Exploration of Causation Hypotheses and Control Methods," in *Proceedings of the ASHRAE/SOEH Conference IAQ* , San Diego, California, April 17-20 1989.

[6] WHO, "Indoor Air Pollutants: Exposure and Health Effects," World Health Organization, 1983.

[7] EN 15251:2007, "Indoor Environmental Input Parameters for Design and Assessment of Buildings Addressing Indoor Air Quality, Thermal Environment, Lighting and Acoustics," European Committee for Standardization, 2007.

[8] S. A. Mumma, "Designing Dedicated Outdoor Air Systems," *Ashrae Journal,* 2001.

[9] B. W. Olesen, "Radiant Floor Cooling Systems," *Ashrae Journal,* 2008.

[10] P. Jacobs, E. C. van Oeffelen and B. Knoll, "Diffuse Ceiling Ventilation, a New Concept for Healthy and Productive Classrooms," TNO Built Environment and Geosciences, Delft, 2008.

[11] C. A. Hviid and S. Svendsen, "Experimental and Numerical Analysis of Perforated Suspended Ceiling as Diffuse Ventilation Air Inlets".

[12] C. A. Hviid and S. Terkildsen, "Experimental Study of Diffuse Ceiling Ventilation in a Classroom," Technical University of Denmark.

[13] T. Mikeska and S. Svendsen, "Study of Thermal Performance of Capillary Micro Tubes Integrated into the Building Sandwich Element Made of High Performance Concrete," *Applied Thermal Engineering,* no. 52, pp. 576-584, 2013.

[14] P. Simmonds, S. Reuss and W. Gaw, "Using Radiant Cooled Floors to Condition Large Spaces and Maintain Comfort Conditions," *Ashrae Journal,* 2000.

[15] S. A. Mumma, "Ceiling Panel Cooling Systems," *Ashrae Journal,* 2001.

[16] J. Dieckmann, K. W. Roth and J. Brodrick, "Radiant Ceiling Cooling," *Ashrae Journal,* 2004.

[17] A. Heller, "Large-Scale Solar Heating- Evaluation, Modelling and Designing," Technical University of Denmark, 2000.

[18] Sensor-electronic, "AirDistSys 5000 product datasheet," [Online]. Available: http://www.sensor-electronic.pl/pdf/KAT_AirDistSys5000.pdf. [Accessed 1 July 2014].

[19] Onset, "HOBO Data Loggers Product Datasheet," [Online]. Available: http://www.onsetcomp.com/products/data-loggers/u12-012. [Accessed 1 July 2014].

[20] EN ISO 7730:2005, "Ergonomics of the Thermal Environment: Analytical Determination and Interpretation of Thermal Comfort Using Calculation of the PMV and PPD Indices and Local Thermal Comfort Criteria," International Organization for Standardization, Geneva, 2005.

[21] Ansys Fluent, "Product Datasheet," [Online]. Available: http://ansys.com/Products/Simulation+Technology/Fluid+Dynamics/Fluid+Dynamics+Products/ANSYS+Fluent . [Accessed 1 July 2014].

[22] T. Mikeska and J. Fan, "Full Scale Measurements and CFD Simulations of Diffuse Ceiling Inlet for Ventilation and Cooling of Densely Occupied Rooms," *Energy and Buildings,* 2014.

[23] W. Vieser, T. Esch and F. Menter, "Heat Transfer Predictions Using Advanced Two-equation Turbulence Models," Ansys, CFX Validatin Report.

[24] Ansys 14.5, "Fluent Theory Guide 4.3.2".